EPJ Web of Conferences **84**, 04004 (2015)
DOI: 10.1051/epjconf/20158404004

ab initio R-matrix and MQDT investigation of low-lying Rydberg states of the HeH^+ molecular ion

I. Bouhali[1], S. Bezzaouia[1], M. Telmini[1,a] and Ch. Jungen[2,3]

[1] LSAMA Departement of Physics, Faculty of Science of Tunis, University of Tunis El Manar, 2092 Tunis, Tunisia
[2] Laboratoire Aimé Cotton du CNRS, Université de Paris-Sud, 91405 Orsay, France
[3] Department of Physics and Astronomy, University College London, London WC1E 6BT, UK

Abstract. We report R-matrix calculations of low-lying Rydberg states of the hydrohelium molecular ion HeH^+ corresponding to $^1\Delta$ and $^3\Delta$ symmetry. The calculations include states with principal quantum numbers $3 \leq n \leq 10$. For $n = 3$ and $n = 4$ the present results are compared with those of Green *et al.* [1, 2] and Loreau *et al.* [3].

1. Introduction

Many theoretical and experimental studies have been devoted to the hydrohelium ion, HeH^+, both because of its role in the early universe [4] and the peculiar vibronic mechanism "without curve crossing" [5, 6] that induces its dissociative recombination (DR) upon collision with slow electrons. Numerous excited states of this ion have been computed from first principles in many studies. We mention here specifically two CI studies dealing with excited states of HeH^+. Green, Michels and collaborators [1, 2, 7, 8] carried out extensive and well-documented calculations back in the 1970's in a valence-bond framework, in the perspective of interpreting helium $\sim$ proton collisions over a large range of energies and interatomic distances. Quite recently, Loreau *et al.* [3] applied the widely used MOLPRO package to the computation of several dozens of HeH^+ potential energy curves with the aim to provide adiabatic as well as diabatized potential curve representations.

The present work is concerned with the calculation of electronically bound low-lying and Rydberg states of HeH^+ based on our implementation of the variational R-matrix method for two-electron systems, the so-called "halfium" code [9, 10]. In general, R-matrix calculations of bound molecular electronic states have remained limited to a handful of species [11]. The UK R-matrix code was used in the 1990's by Sarpal *et al.* [12] to address the problem of low-lying and Rydberg states of neutral HeH. In that work 11 known states of HeH were reproduced with a mean deviation of $140\,cm^{-1}$, and many predictions of higher states were made. A few years later an effective one-electron variational R-matrix "ligand field" approach was used [13] to study the bound states of the related systems ArH and KrH, giving less accurate results for these many-electron systems, but which were comparable with

[a]Corresponding author: mourad.telmini@fst.rnu.tn

the then best available quantum-chemical computations (for ArH only). Our aim here is to test the use of the "halfium" code in a heteronuclear molecule, and to compare our results with existing CI potential energy curves [1–3], while also making predictions of higher states that have not been studied so far. We choose the $^1\Delta$ and $^3\Delta$ states of HeH^+ for this purpose.

2. Theory

The "halfium model" combines the R-matrix theory with generalized multichannel quantum defect theory (GMQDT). It is set up in spheroïdal coordinates in view of an efficient description of two-center systems. In the spirit of R-matrix theory, the configuration space is divided into two regions: (i) an internal or "reaction" zone, where the short-range interactions take place and a two-electron clamped-nuclei CI treatment is carried out with an appropriate variational basis set, and (ii) an external or "asymptotic" zone, where it is assumed that the outermost electron is moving in the field of the residual ion core and a one-electron picture is appropriate. The reaction volume is an ellipsoid with the nuclei placed in the focal positions and separated by the internuclear distance R.

For these assumptions to be valid, the reaction volume must be chosen large enough so that it contains the relevant target states. In our case these will be the two lowest states of HeH^{++}, $1s\sigma$ and $2p\sigma$, which shall serve as target states for the description of the motion of the outermost electron in the asymptotic zone. The boundary is defined by $\max(\xi_1, \xi_2) = \xi_0$ where ξ denotes the spheroïdal radial coordinate. In this work we parametrize ξ_0 according to $\xi_0 = 1 + C/R$ with $C = 12$ a.u., and we have checked that with this choice the confined wavefunctions of the $1s\sigma$ and $2p\sigma$ core states yield energies to within 10^{-3} a.u. of those of the free ion core.

Figure 1 is a color-coded plot of the squared $1s\sigma$ wavefunctions for H_2^+ (left) and HeH^{++} (right) for two values of the bond length, $R = 1$ ($\xi_0 = 13$) and 5 a.u. ($\xi_0 = 3.4$), respectively. The abscissa corresponds to the spheroïdal angular coordinate $-1 \le \eta \le 1$, and the ordinate to the spheroïdal radial coordinate $\xi \ge 1$. The nuclear positions (ξ, η) thus correspond to (1,-1) and (1,1) for He^{++} (H^+) and H^+ (H^+) in the two systems, respectively. It is at once obvious how in the doubly charged ion HeH^{++} the probability density decreases much faster with increasing ξ than in the singly charged ion H_2^+. The dipolar nature of HeH^{++} also emerges clearly, with almost no electronic probability density left on the proton for $R = 5$ a.u.

A key point of our approach is that we use a spheroïdal representation in both the internal and the external zone of the configuration space. Specifically, our implementation in terms of regular and irregular channel functions follows exactly the definitions and procedures described in Refs. [14, 15] for dipolar two-center systems. In the variational calculation in the inner zone the two-electron wavefunction is expanded in terms of a variational basis consisting of antisymmetrized products of eigenfunctions of HeH^{++} that take also account of the σ_v symmetry [16, 17]. The only changes with respect to our previous applications to H_2 is that here we use nuclear charges $Z_1 = 2$ and $Z_2 = 1$ instead of $Z_1 = Z_2 = 1$, and we include simultaneously even as well as odd ℓ values in the variational basis.

The choice of Z_1 and Z_2 for the channel functions in the asymptotic zone requires somewhat more thought. In H_2, the obvious choice is to take fractional charges $Z_1 = Z_2 = 1/2$ on each center (whence the denomination "halfium" [9]), because we must have $Z_1 + Z_2 = 1$ and the molecule is symmetric. This way of accounting for the partial screening by the core electron has the advantage that it provides a realistic approximation to the quadrupole field outside the ion core, which therefore is directly taken into account in the asymptotic channel functions [18]. In HeH^+ we must have $Z_1 + Z_2 = 2$, but the distribution of the total charge on the two centers is *a priori* arbitrary and in fact, strictly speaking, irrelevant. Any converged calculation should yield the same result whatever choice has been made, although the ℓ-mixing channel interactions will be different and the convergence properties may not be the same.

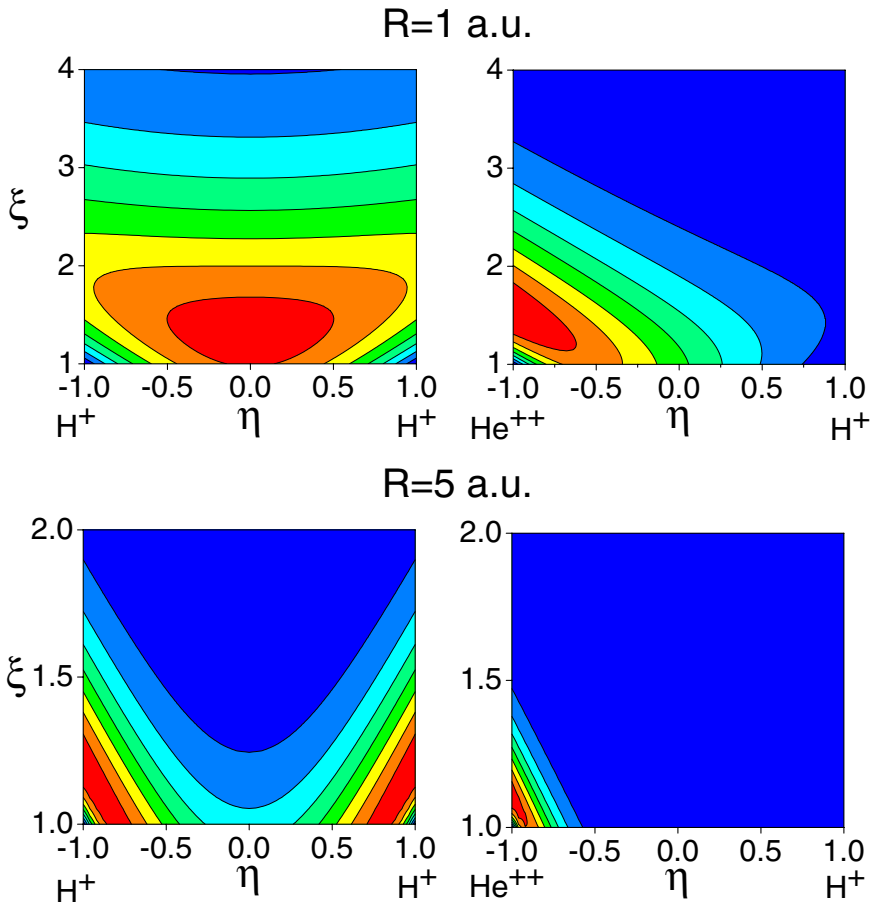

Figure 1. Comparison of the probability densities of the H_2^+ (left) and HeH^{++} (right) $1s\sigma$ orbital for $R = 1$ a.u. (top) and $R = 5$ a.u. (bottom). The probability density scale is arbitrary with the density decreasing from red to blue.

For instance we may distribute the total charge in such a way that at very large distance ξ from the core the outermost electron sees a double point charge situated on the center of charge of the ion core. The advantage of this choice would be that the dipole component of the longe-range field vanishes [19], and therefore dipolar channel couplings are minimized, and – hopefully – the convergence is faster. This choice is dependent on the internuclear distance R, but since HeH^{++} quickly approaches the configuration $He^+ + H^+$ (cf. Fig. 1) the center of charge will be near the midpoint between the two nuclei, implying $Z_1 = Z_2 = 1$. Another possible choice is the following: if we are interested in spectroscopic applications of the computed reaction **K** or quantum defect μ matrices we should choose the center of mass as origin in order to achieve the separation of translation from the rotational motion. This means that at large distance the outermost electron experiences a double charge situated at the center of mass, which for $^4HeH^+$ implies $Z_1 = 8/5$ and $Z_2 = 2/5$ elementary charges for all values of R. Yet another choice consists in taking $Z_1 = 4/3$ and $Z_2 = 2/3$, implying that the fractional charges are distributed on the two centers in the same way as on the bare nuclei. In the present work we have carried out two sets of calculations with two different choices, namely $Z_1 = Z_2 = 1$ and $Z_1 = 4/3$ and $Z_2 = 2/3$. This procedure allows us to check the convergence of the angular basis employed because

Table 1. Comparison of calculated effective quantum numbers for $^1\Delta$ $n\tilde{d}\delta$ states of HeH^+ with those from Refs. [1] and [3].

		$3\tilde{d}\delta$			
R(a.u.)	$\nu_{present}$	Ref. [1]	Ref. [3]	$\Delta\nu$[1]	$\Delta\nu$[3]
1.0	3.0185	3.0382	3.2027	−0.0197	−0.1842
2.0	3.0668	3.0733	3.2949	−0.0065	−0.2281
3.0	3.1318	3.1352	3.3607	−0.0034	−0.2289
4.0	3.2071	3.2098	3.4239	−0.0027	−0.2168
5.0	3.2869	–	3.4857	–	−0.1988
mean deviation	–	–	–	−0.0081	−0.2114
in cm^{-1}	–	–	–	−66	−1718
		$4\tilde{d}\delta$			
R(a.u.)	$\nu_{present}$	Ref. [1]	Ref. [3]	$\Delta\nu$[1]	$\Delta\nu$[3]
1.0	4.0203	4.0605	4.4723	−0.0402	−0.4520
2.0	4.0734	4.0763	4.7075	−0.0029	−0.6341
3.0	4.1391	4.1333	4.7893	0.0058	−0.6502
4.0	4.2117	4.2057	4.8409	0.0060	−0.6292
5.0	4.2890	–	4.8809	–	−0.5919
mean deviation	–	–	–	−0.0078	−0.5915
in cm^{-1}	–	–	–	−27	−2028

	$5\tilde{d}\delta$	$6\tilde{d}\delta$	$7\tilde{d}\delta$	$8\tilde{d}\delta$	$9\tilde{d}\delta$	$10\tilde{d}\delta$
R(a.u.)	$\nu_{present}$	$\nu_{present}$	$\nu_{present}$	$\nu_{present}$	$\nu_{present}$	$\nu_{present}$
1.0	5.0199	6.0197	7.0196	8.0195	9.0194	10.0194
2.0	5.0716	6.0706	7.0700	8.0698	9.0696	10.0694
3.0	5.1356	6.1336	7.1326	8.1321	9.1317	10.1315
4.0	5.2059	6.2030	7.2015	8.1993	9.1993	10.1992
5.0	5.2807	6.2766	7.2744	8.2730	9.2724	10.2711

we know that we should obtain the same results with either choice. Apart from the differences just mentioned, the present application of the variational R-matrix procedure closely follows the descriptions given in Refs. [9, 10]. It is the matching of the solutions obtained inside and outside the reaction volume that yields the short-range reaction matrix **K** and quantum defect matrix μ, based on which bound states are determined with standard MQDT procedures.

3. Application to $^{1,3}\Delta$ states of the HeH^+ ion

The basis sets used for the description of the wavefunction inside are basically similar as in the previous applications (see Refs. [9, 10]) except that they are effectively twice as large here because there is no *gerade/ungerade* classification of states. In the asymptotic zone we include two core-ground state channels, $(1\tilde{s}\sigma)\epsilon\tilde{d}\delta$ and $(1\tilde{s}\sigma)\epsilon\tilde{f}\delta$, and two core-excited channels, $(2\tilde{p}\sigma)\epsilon\tilde{d}\delta$ and $(2\tilde{p}\sigma)\epsilon\tilde{f}\delta$. Note that we use here the notation $n\tilde{\ell}\lambda$ for labeling the core wavefunctions and Rydberg channels, with the tilde on ℓ designating the spheroïdal orbital angular momentum, not to be confused with its spherical analog [14]. The variational basis included 300 to 400 "closed" functions (that vanish on the reaction boundary), depending on the R-value, with two "open-type" basis functions (whose derivative vanishes on the reaction boundary) added for each asymptotic channel. We have found that the present angular basis with the two choices of Z_1 and Z_2 gives results that agree to within less than 1 meV for the $3\tilde{d}\delta$ states

Table 2. Comparison of calculated effective quantum numbers for $^3\Delta$ $n\tilde{d}\delta$ states of HeH^+ with those from Refs. [2] and [3].

		$3\tilde{d}\delta$			
R(a.u.)	$\nu_{present}$	Ref. [2]	Ref. [3]	$\Delta\nu$[2]	$\Delta\nu$[3]
1.0	3.0160	3.0343	3.2031	−0.0183	−0.1871
2.0	3.0645	3.0696	3.2928	−0.0051	−0.2283
3.0	3.1302	3.1348	3.3582	−0.0046	−0.2280
4.0	3.2058	3.2081	3.4216	−0.0023	−0.2158
5.0	3.2857	3.2869	3.4835	−0.0012	−0.1978
mean deviation	–	–	–	−0.0063	−0.2114
in cm^{-1}	–	–	–	−51	−1718
		$4\tilde{d}\delta$			
R(a.u.)	$\nu_{present}$	Ref. [2]	Ref. [3]	$\Delta\nu$[2]	$\Delta\nu$[3]
1.0	4.0174	4.0555	–	−0.0381	–
2.0	4.0704	4.0724	–	−0.0020	–
3.0	4.1371	4.1352	–	0.0019	–
4.0	4.2101	4.2036	–	0.0065	–
5.0	4.2870	4.2783	–	0.0087	–
mean deviation	–	–	–	−0.0046	–
in cm^{-1}	–	–	–	−16	–

	$5\tilde{d}\delta$	$6\tilde{d}\delta$	$7\tilde{d}\delta$	$8\tilde{d}\delta$	$9\tilde{d}\delta$	$10\tilde{d}\delta$
R(a.u.)	$\nu_{present}$	$\nu_{present}$	$\nu_{present}$	$\nu_{present}$	$\nu_{present}$	$\nu_{present}$
1.0	5.0166	6.0162	7.0160	8.0159	9.0158	10.0157
2.0	5.0682	6.0670	7.0664	8.0661	9.0658	10.0657
3.0	5.1330	6.1308	7.1298	8.1292	9.1288	10.1286
4.0	5.2040	6.2009	7.1994	8.1984	9.1977	10.1973
5.0	5.2784	6.2741	7.2718	8.2703	9.2695	10.2687

and to within less than 4 meV for the $4\tilde{d}\delta$ for R ranging from 1 to 5 a.u. By contrast, in the case of the $\tilde{f}\delta$ states with $n = 3$ and 4 the differences are also quite small for $R = 1$ and 2 a.u., but increase rapidly for higher R values indicating that the present angular basis is insufficient for these higher $\tilde{\ell}$ states. We therefore report only the $n\tilde{d}\delta$ states in the present paper.

Tables 1 and 2 contain our results obtained with the choice $Z_1 = Z_2 = 1$ and compare them with previous calculations [1–3]. We have chosen to list effective principal quantum numbers ν_n rather than the absolute energies of the electronic potential energy curves $U_n(R)$ which we initially obtain. The former are related to the latter by the Rydberg equation

$$\nu_n(R) = \sqrt{\frac{Z_{core}^2}{2[U^+(R) - U_n(R)]}}, \tag{1}$$

where U_n and U^+ are in a.u.. $U^+(R)$ is the potential energy curve of the HeH^{++} ground state which is calculated essentially exactly because the HeH^{++} one-electron problem is separable in the spheroïdal coordinate system which we use here. $Z_{core} = 2$ denotes the total charge of the HeH^{++} core. The use of $\nu_n(R)$ instead of $U_n(R)$ makes it easier to recognize the regularity of Rydberg series as functions of the principal quantum number n and the internuclear distance R, and to assess the constancy of the quantum defects $\mu = n - \nu$. Further, penetrating series may be readily distinguished from non-penetrating ones

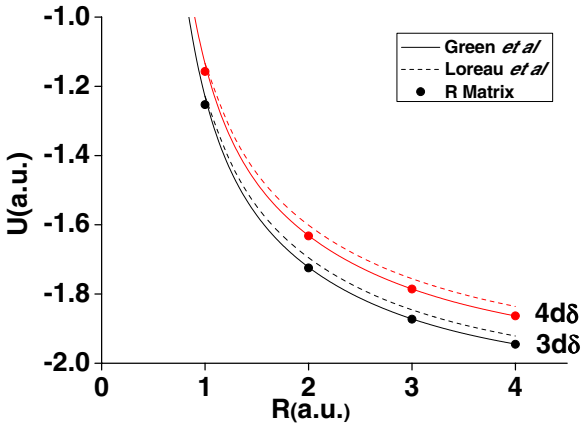

Figure 2. Clamped-nuclei potential energy curves of the $3\tilde{d}\delta$ (black symbols) and $4\tilde{d}\delta$ (red symbols) $^1\Delta$ states of the HeH^+ ion. The present results (dots) are compared with those of Refs. [1] (solid line) and [3] (dashed line).

as the latter are characterized by small quantum defects, $|n - \nu| \ll 1$. The electronic $n\tilde{d}\delta$ states of HeH^+ do of course not correspond to pure $\tilde{d}$ Rydberg states but they are labeled in Tables 1 and 2 according to the main component in the multichannel wave function. Inspection of the eigenvectors obtained in the MQDT calculations indicates that in fact (depending on the choice of Z_1 and Z_2 [see Sect. 2]) there is always some $\tilde{d}\delta \sim \tilde{f}\delta$ mixing present.

Table 1 lists the results for the $n\tilde{d}\delta$ $^1\Delta$ states for $n = 3$ to 10, while Table 2 provides the corresponding information for $^3\Delta$ states. Note that the R-matrix approach allows us to follow up Rydberg series up to arbitrary high-n quantum numbers and into the continuum with no loss of accuracy in principle, but we defer the continuum calculations to a future publication. On the other hand, quantum-chemical CI calculations are still limited essentially to $n \leq 5$ at present, and the results from Refs. [1–3] included in the Tables indeed correspond to this range, whereas we provide a few higher roots. The two Tables contain the values from the earlier references, as well as the differences of our present ν values with respect to the older work. In addition, the mean values of the differences are given for the various sets of ν_n values.

The comparisons that can thus be made for the $^1\Delta$ and $^3\Delta$ states are instructive and indeed somewhat surprising. It turns out that our results for the $n\tilde{d}\delta$ singlet series (Table 1) are in far better agreement with the early work of Green *et al.* [1, 2] than with the latest values of Loreau *et al.* [3]. These latter authors mention difficulties in the application of the MOLPRO package to Δ states, however without making any detailed comparisons with the earlier work. We therefore focus our comparison with earlier work on Refs. [1, 2] for the two states $3\tilde{d}\delta$ and $4\tilde{d}\delta$ for $R = 1 - 5$ a.u.. For these states we find agreement to within about $50\,cm^{-1}$, which is somewhat better than that reached previously for H_2 $^1\Sigma_g$, $^1\Pi_g$, $^1\Delta_g$ states [10], and comparable to the accuracy achieved for HeH in Ref. [12]. Note that our ν values – and hence total energies – are with few exceptions somewhat lower than those from Refs. [1, 2]. The $3\tilde{d}\delta$ and $4\tilde{d}\delta^1\Delta$ potential curves are shown in Fig. 2. Our values (dots) and those of Green *et al.* [1] (solid lines) for $n = 3$ are seen to lie significantly lower than the MOLPRO results [3] (dashed lines).

4. Discussion

Figure 3 displays the evolution with R and n of the quantum defects $\mu_n(R) = n - \nu_n(R)$ [where $\nu_n(R)$ is given by Eq. (1)]. The quantum defects are seen to have negative values which increase substantially with increasing internuclear separation. The dependence of the quantum defect on the principal quantum

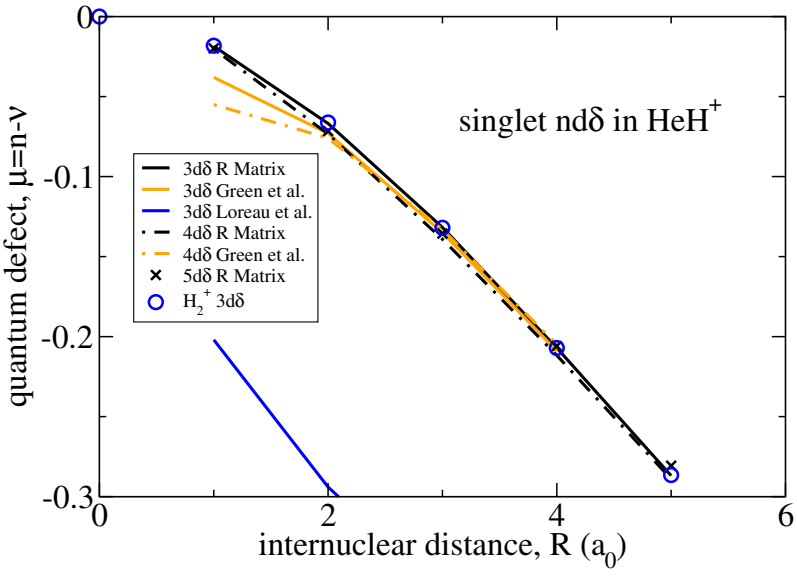

Figure 3. Quantum defects for $^1\Delta$ symmetry ($\tilde{d}\delta$ wave) in HeH^+ plotted as function of the internuclear distance R for various principal quantum numbers n. The meaning of the symbols is indicated in the figure.

number (and hence the energy) on the other hand is predicted to be small. Only values up to $n = 5$ have been included in the figure for clarity, but the data given in Table 1 show that the values for n up to 10 line up nicely with the lower values. The good agreement with the results of Ref. [1] and striking discrepancy with those of Ref. [3] is again apparent.

The strong tendency of the quantum defects towards negative values is directly related to the fact that the doubly charged ion core dissociates into two charged fragments, as we now show. Indeed, in the situation considered here the HeH^{++} core dissociates into two particles with $Z_d = 1$ and the Rydberg electron will be bound to one of them with an asymptotic Rydberg energy $-Z_d^2/(2\nu_d^2)$ (in atomic units). Since we derive the quantum defects by use of Eq. (1) we have the formal relationship

$$\frac{Z_{core}^2}{2\nu^2} = \frac{Z_d^2}{2\nu_d^2} \quad (R \to \infty)\,, \tag{2}$$

where ν_d is the effective principal quantum number of the Rydberg electron in the fragmented system. This implies that

$$\nu(R \to \infty) = \frac{Z_{core}}{Z_d}\nu_d, \tag{3}$$

where in the problem at hand we have $Z_{core} = 2$ and $Z_d = 1$. Therefore, assuming that the $3\tilde{d}\delta$ singlet and triplet states dissociate with $\nu_d = 3$, we find that $\nu(R \to \infty) = 2\nu_d = 6$ implying that the quantum defect formally converges towards the value -3. The $R-$ dependence of the quantum defects seen in Fig. 3 represents just the beginning of this evolution which is a purely electrostatic effect not present in the Rydberg states of neutral molecules where $Z_d = Z_{core}$ in Eq. (3). It is interesting to test the hypothesis made in Sect. 2 that the molecular core HeH^{++} quickly approaches the configuration $He^{++}H^+$ as R increases. In that event the two-electron system HeH^+ reduces to an effective one-electron system equivalent to H_2^+. The effective principal quantum numbers then approach those of H_2^+ evaluated with

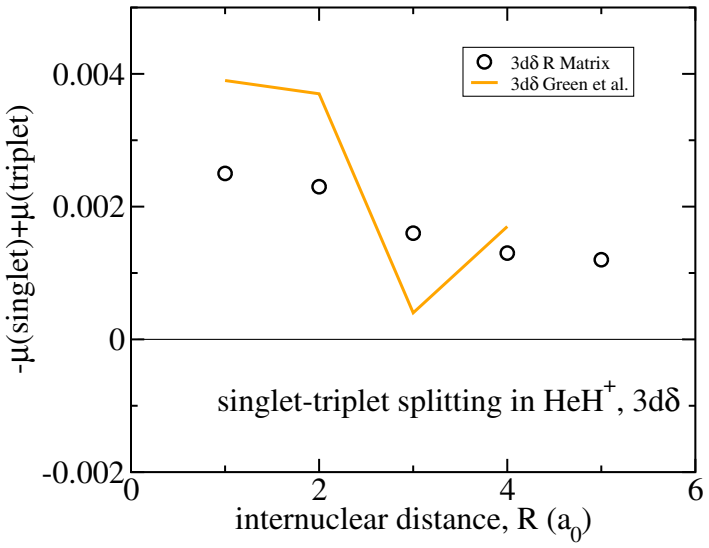

Figure 4. Singlet-triplet splitting in the $3\tilde{d}\delta$ state of HeH^+. The quantity plotted is ν(singlet)-ν(triplet) $\equiv$ $-\mu$(singlet)+μ(triplet) as a function of R. The meaning of the symbols is indicated in the figure.

Eq. (1), where $U_n(R)$ is replaced by the exact H_2^+ energy and $U^+(R)$ is replaced by the proton-proton repulsion $+1/R$ a.u. The quantum defects obtained in this manner for $3\tilde{d}\delta$ are plotted in Fig. 3 as blue circles. It may be seen that throughout the range $R = 1 - 5$ a.u. these values are indeed very close to the corresponding values obtained in our R-matrix calculations and in the calculations of Ref. [1].

A measure for the deviation of HeH^+ from this purely electrostatic effective one-electron model is provided by the singlet-triplet splitting of the Δ states which specifically depends on the exchange interaction between the two electrons. This splitting turns out to be very small as is shown by the data collected in Tables 1 and 2. Figure 4 displays the quantity ν(singlet)-ν(triplet) $\equiv$ $-\mu$(singlet)+μ(triplet) for the $3\tilde{d}\delta$ state of HeH^+ as a function of R and compares it with the corresponding information extracted from Refs. [1, 2]. The two sets of data agree qualitatively and appear to corroborate the assumption that the singlet-triplet splitting should decrease and tend to zero as R increases. The splittings are predicted to be quite small – smaller than about 4 meV – and are certainly at the limit of what our R-matrix approach is capable of doing at this stage of development.

5. Conclusion

We have presented R-matrix calculations of low-lying Rydberg states of $^1\Delta$ and $^3\Delta$ symmetry in HeH^+. The adaptation of the "halfium" code to heteronuclear molecules has been discussed. We have compared our results with available *ab initio* data for the same states. It turns out that we have been able to reach the same degree of accuracy as we obtained previously for excited states of H_2 to which we initially applied our code [9, 10]. The comparison with previously published computations on HeH^+ has revealed major discrepancies between Refs. [1, 2] and Ref. [3]. Our computations agree much better with the former than with the latter. In conclusion it appears that the development of novel conceptual and numerical tools for the calculation of electronically highly excited bound and continuous molecular states remains an important issue. The extension of the present work to higher energies, to larger R values, and to the $^{1,3}\Sigma^+$, $^{1,3}\Sigma^-$ and $^{1,3}\Pi$ symmetries of HeH^+ is underway.

Foremost thanks are due to Dr. Martin Jungen (University of Basel) who kindly pointed out inconsistencies in an earlier version of the present manuscript and thereby helped to improve this paper decisively. He also communicated to us his as yet unpublished quantum-chemical calculations on excited states of HeH^+ which fully support our conclusions. We are indebted to Dr. Jérôme Loreau (Brussels) for letting us have his PEC curves of HeH^+ in numerical form. Ch. J. was supported in part by the ANR (France) under Contract No. 09-BLAN-020901. M. T. has received travel support from the same ANR contract. Ch. J. also received funding from the E. Miescher Foundation (Basel, Switzerland).

References

[1] T. A. Green, H. H. Michels, and J. C. Browne, J. Chem. Phys. **64** (1976) 3951
[2] T. A. Green, H. H. Michels, and J. C. Browne, J. Chem. Phys. **69** (1978) 101
[3] J. Loreau, J. Liévin, P. Palmeri, P. Quinet, and N. Vaeck, J. Phys. B. At. Mol. Opt. Phys. **43** (2010) 065101
[4] W. Roberge and A. Dalgarno, Ap. J. **255** (1982) 489
[5] S. L. Guberman, Phys. Rev. A **49** (1994) R4277
[6] B. K. Sarpal, J. Tennyson and L. A. Morgan, J. Phys. B.: At. Mol. Opt. Phys. **27** (1994) 5943
[7] T. A. Green, H. H. Michels, J. C. Browne, and M. M. Madsen, J. Chem. Phys. **61** (1974) 5186
[8] T. A. Green, J. C. Browne, H. H. Michels, and M. M. Madsen, J. Chem. Phys. **61** (1974) 5198
[9] M. Telmini and Ch. Jungen, Phys. Rev. A **68** (2003) 062704
[10] S. Bezzaouia, M. Telmini and Ch. Jungen, Phys. Rev. A **70** (2004) 012713
[11] J. Tennyson, Phys. Rep. **49** (2010) 29
[12] B. K. Sarpal, S. E. Branchett, J. Tennyson and L. A. Morgan, J. Phys. B.: At. Mol. Opt. Phys. **24** (1991) 3685
[13] Ch. Jungen, A. L. Roche and M. Arif, Phil. Trans. R. Soc. Lond. A **355** (1997) 1481
[14] M. Arif, Ch. Jungen and A. L. Roche, J. Chem. Phys. **106** (1997) 4102
[15] Ch. Jungen and F. Texier, J. Phys. B.: At. Mol. Opt. Phys. **33** (2000) 2495
[16] S. Bezzaouia, F. Argoubi, M. Telmini and Ch. Jungen, J. Phys.: Conf. Ser. **300** (2011) 0123013
[17] F. Argoubi, S. Bezzaouia, H. Oueslati, M. Telmini and Ch. Jungen, Phys. Rev. A **83** (2011) 052504
[18] S. Bezzaouia and M. Telmini, AIP Conf. Proc. **935** (2007) 183
[19] J. K. G. Watson, Molec. Phys. **81** (1994) 277